Flow of Noncolloidal Slurries in Pipelines

A multiphase model for the flow of dense, noncolloidal, settling slurries through horizontal pipelines, and an associated Galerkin-finite element numerical scheme to carry out computer simulations based on the model, were developed. The principal elements of the model are: equations for estimation of the velocity distributions for each component; and those for the concentration distributions. In the former, which are derived from the local volume-averaged, time-smoothed conservation of mass and momentum equations, the total stress is comprised of components to account for interparticle and particle-boundary as well as viscous and turbulent interactions. The governing equations for the concentration distributions are derived similarly from the convective diffusion equation, with the eddy diffusivity modified to account for the presence of the solid particles. Numerical simulations and detailed comparisons with experiment for the flow of gypsum, coal, crushed glass, sand and gravel, covering particle sizes from 38.3 μm to 13,000 μm, and pipe diameters from 4 cm to 49.5 cm, were carried out. The agreement between model prediction and experiment is excellent.

Feng-Lung Hsu
Raffi M. Turian
Tzu-Wang Ma
Department of Chemical Engineering
University of Illinois
Chicago, IL 60680

Introduction

The applications of transport of solids by liquids in pipelines are broad. They include long distance hauling of coal, minerals, ore and solid commodities, dredging and filling, collection and disposal of solid waste and materials processing. A distinguished class of suspended particle systems consists of concentrated slurries containing coarse, dense particles. Virtually all suspended systems encountered in slurry pipelines transportation and a substantial fraction of all industrial slurries belong to this class. The present study is concerned mainly with this type of solid-liquid mixture.

The problem considered in this work is the formulation of a model capable of predicting the *in-situ* velocity and concentration distributions for all components as well as the pressure gradient and holdup, for the flow of dense, noncolloidal, settling slurries through horizontal pipelines and the development of an appropriate numerical scheme to carry out numerical simulations based on the model. A slurry system is specified when the pertinent physical properties of the solid and liquid components are given and when the operating conditions and pipe size are prescribed. The basic properties are the densities and particle sizes of the solid components, the density and viscosity of the carrier liquid, and the maximum packing concentration of solids. The operating conditions are taken as the average discharge slurry velocity and the average discharge solids concentration.

The present slurry flow model is applicable strictly to noncolloidal slurries, because nonhydrodynamic double-layer particle interaction effects are not accounted for, since definitive expression of such effects within the complex flow field which prevails here is not presently possible. Nevertheless, the particle size limits of the present slurry model are broad and include suspensions of particles fine enough to be capable of meaningful rheological characterization. Such fine particulate suspensions provide a test of the present multiphase flow modeling approach against the continuum rheological approach for predicting slurry flow behavior.

Previous Work and Background Data

Studies concerned with solid-liquid mixture flows have followed one of these three major approaches:

1) The empirical approach
2) The rheologically-based continuum approach
3) The multiphase flow modeling approach

The empirical correlation approach seems to have received the most attention, certainly early on, almost surely as a concession to the mathematical complexity of slurry flows. Because of its long history, a large body of empirical studies dealing with slurry transport has accumulated. Correlations for prediction of

Correspondence concerning this paper should be addressed to R. M. Turian.

pressure drops (Kazanskij, 1978) and for delineation of flow regimes (Turian and Yuan, 1977) constitute two major elements of this body of empirical work.

The rheologically-based approach seems to have emerged in a major way in the mid-fifties (Metzner and Reed, 1955; Dodge and Metzner, 1959). For noncolloidal slurries it is strictly applicable to fine, slowly settling suspensions capable of meaningful rheological characterization. It is inevitably used with colloidal particle dispersions because a rigorous mathematical particle dynamics approach accounting for colloidal nonhydrodynamic interactions is out of reach at present.

For slurries containing coarse particles, the concept of viscosity is meaningless. The multiphase flow modeling approach, which accounts for liquid, particle and boundary interaction effects, provides the most rational framework for describing such heterogeneous solid-fluid mixture flows. It requires basic information regarding the effects of the particles on the structure of the turbulent flow, the particle-particle and the particle-boundary interactions, and other effects, and the approach commonly entails substantial computational effort. Perhaps because of this, studies utilizing the multiphase flow modeling approach for describing slurry transport did not attain great momentum until the late seventies, despite some pioneering work, notably that due to Tchen (1947) some three decades before.

Development of multiphase flow models of slurry transport

The motion of materials consisting of particles dispersed in a continuous fluid phase has been described using both Lagrangian and Eulerian formulations. In the Lagrangian description, the motions of the individual particles are calculated and relevant properties of the flow are then computed by integration along the particle trajectories. In the Eulerian description, the multiphase flow is viewed as a system of multiple interacting continua, with individual boundary conditions appropriate to each phase. The properties of the solid phases are not calculated along particle trajectories, but are obtained by solving equations pertaining to the local mean bulk properties of the individual components and the mixture.

One of the earliest, and most cited, treatments of multiphase flow using the Lagrangian approach is that due to Tchen (1947), which is summarized by Hinze (1975). More recent investigations following this approach are those due to Lee and Durst (1982) and Ormancey and Martinon (1984) dealing with the analysis of particle deposition rates on walls from turbulent pipe flow and the prediction of particle dispersion in turbulent flow, respectively.

Studies utilizing the Eulerian approach can be roughly classified into two categories. In the first, the multiple phases are viewed as separate, interacting continua, in which dispersion or convective transport of the solid components is considered. Formulations using this approach have been given by Drew (1976), Kril' (1981) and Pourahmadi and Humphrey (1983). The multiphase slurry flow model developed in this study belongs to this category. In the second category, the multiphase mixture is viewed as a whole with the bulk properties modified to account for the presence of the solid components. Studies utilizing this approach include those due to Wallis (1969) and Hinze (1972). However, the major works concerned with slurry flow here have been done by Roco and his coworkers (Roco and Shook, 1983, 1985; Roco and Mahadevan, 1986). It should be mentioned that Roco and his coworkers do formulate the equations of motion for each component of an N-component mixture, but they also carry out calculations based upon summing the equations over all components, which results in the equation for the mixture (Roco and Shook, 1985; Roco and Mahadevan, 1986).

These various approaches of treating multiphase flow are not incompatible. The success of any one approach in providing an effective description of the multiphase flow process depends upon the appropriate inclusion and the accurate modeling of the various complex effects in the governing equations. Therefore, a successful predictive model must be based on a solid understanding of the fundamentals of particle-laden turbulent flows, including all significant interactions, and the ability to integrate these quantitatively into an appropriate model. The presence of solids affects the turbulent flow in a complex way. Owen (1969) has observed that increasing particle concentration results in reduction of fluid turbulence intensity. On the other hand, Soo et al. (1960) observed no such effect due to the presence of particles. Kada and Hanratty (1960), Hino (1963), and Owen (1969) have reported that increasing particle concentration results in an increase in the rate of dissipation of turbulent kinetic energy. However, the latter two investigators and Pechenkin (1972) have found that increasing particle concentration results in a decrease in eddy diffusivity, in contrast with the observations of Kada and Hanratty (1960). Zisselmar and Molerus (1979), using laser Doppler anemometry, found that the intensity of turbulence is profoundly affected by the presence of the particles—the particles increasing or dampening turbulence intensity depending upon solids concentration and also upon distance from the wall. Keska (1984) found that the fluctuation amplitude of the solids concentration increased as the mixture velocity decreased, attaining some maximum amplitude value. Beyond this, further decrease of the mixture velocity resulted in decrease in amplitude until the dynamic component disappeared entirely close to the critical velocity. The fluctuation frequency, however, was found to increase steadily with increasing mixture flow velocity and to decrease with increasing particle size. More recently, Soo (1987) observed that particle diffusivity and the relative motion among particles are more pronounced for dilute suspensions than for dense suspensions.

In spite of the lack of detailed fundamental knowledge required for the formulation and modeling of multiphase turbulent flows, the need to predict flows of slurries of industrial interest has motivated work aimed at obtaining approximate solutions. Danon et al. (1977) have presented a model for two-phase turbulent flows which is based on the conservation of mass and momentum. In this model, the solid-phase velocity is not calculated directly but is assumed to be equal to the fluid velocity. As a simplification, particle-particle and particle-wall effects were not considered. Genchev and Karpuzov (1980) have proposed a turbulence model for fluid-solid mixture flows in which the presence of particles in the turbulent transport equations is considered. The assumptions of uniform solids concentration and equality of solid and fluid velocities simplifies the problem; equations for solid phase concentration and velocity are not needed. Pourahmadi and Humphrey (1983) have presented a two-dimensional two-phase flow model for dilute ($C \ll 1$) particulate flows in which the flow variables are obtained using a two-equation ($k - \epsilon$) model of turbulence for each phase, but without including particle-particle interaction effects. Roco and Shook (1983) proposed the support load concept to account for

the particle-particle and particle-wall interaction effects. They treated the solid-fluid mixture as a single continuum and empirically redefined the dynamic viscosity of the mixture. The Reynolds stresses were calculated using a zero-order turbulent model [i.e., using a turbulent coefficient, see Roco and Shook (1983)] together with the assumption of negligible slip velocities. They also presented a new method for estimating the concentration profiles based on a force balance in the gravitational direction. In general, calculated results seemed to agree well with experiment. Since then, Roco and Balakrishnam (1985) and Roco and Mahadevan (1986) extended these calculations by using a more elaborate turbulent model (ϵ- or k-equation) to estimate the Reynolds stresses of the mixture, albeit without further improvement in the results. The relative velocity between each solid component and the mixture is calculated by invoking an analogy with terminal velocity in gravitational sedimentation (Mahadevan, 1984). It is not obvious that such a procedure can account adequately for such effects as the solid-solid and solid-fluid interactions. Roco and Mahadevan (1986) used a force balance in the axial direction on the assembly of particles within a finite volume to estimate the relative velocity. In their calculation, the solid-solid interaction arising from the velocity difference is not considered.

The majority of the analytical treatments for calculation of the concentration distribution are based on the concept of convective diffusion. Such models, being kinematic in nature, provide a description of the distribution of the suspended particles provided the concentration at a reference point is prescribed.

O'Brien (1933) assumed a balance between the rate of settling of particles and the rate of their upward transport by turbulent forces, and stated that

$$\epsilon \frac{dC}{dy} + \omega C = 0 \tag{1}$$

where ϵ is a sediment transfer coefficient and ω is the terminal velocity of particles. In analogy with the turbulent kinematic viscosity coefficient, ν_t, ϵ may be expressed as a function of position, the von Kármán universal constant, κ, and the friction velocity, v_*. It is found, however, that κ is a function of solids loading; decreasing with increasing loading due to the damping effect of the solids on the turbulent eddies.

Shook and Daniel (1965) explain deviations between observed concentration profiles and those calculated by Eq. 1 by postulating that a normal dispersive force, P_B, is associated with the shear stress. This is the so-called Bagnold force (Bagnold, 1954). Recently, Scarlett and Vinhas (1984) have applied diffusion theory with experimentally determined values for the effective solid diffusion coefficient to solve for the concentration profiles in circular and triangular pipes. Bechteler and Farber (1985) developed a stochastic model for suspended solid dispersion in turbulent open channel flow. The local concentration of solids is determined using Monte Carlo methods and random walk calculations, and the equivalence between the stochastic approach and the diffusion equation is considered.

Roco and Shook (1983, 1985) approximated the upward turbulent drag force applied to a cloud of solid particles by assuming the kinetic energy term to be defined in terms of the settling velocity $\omega(C)$, calculated from Eq. 1, and the drag coefficient to be defined in terms of the hindered settling velocity, calculated using Richardson and Zaki's (1954) correlation. Equation 1 and Richardson and Zaki's equation provide the scheme for incorporating the concentration within a force balance involving the turbulent drag force, the dispersive force, the Coulombic normal force, and the net gravitational force, which constitutes a computational form for determining solids concentration. Of course, the accuracy of the results will depend, at least in some measure, upon how well the simplified form in Eq. 1 is capable of accounting for the effects of solids concentration.

Formulation of Slurry Flow Model

Overall description of slurry flow model

The model for slurry flow in pipelines consists of two main elements: equations for estimation of the velocity distributions for each of the slurry components; and equations for estimation of the concentration distributions. These equations are coupled.

The governing equations for the velocity distributions are derived by application of the conservation of mass and momentum. Unlike the case for single-phase flow, the momentum equation contains two extra terms to account for interactions among solid components and between the solid and liquid phases. The inclusion of the solid-solid interaction term, which arises from the difference in solid component velocities, and which, to our knowledge, has not been included in previous formulations of the momentum equations, enables us to calculate the velocity profiles for the individual components in multicomponent slurry flows. The total stress contains a component to account for the Coulombic friction among contacting solids in addition to the viscous and turbulent components. In the present formulation, we use a so-called zeroth-order turbulent model. A zeroth-order model has previously been used also by Roco and Frasineanu (1977). We propose a new method to estimate the eddy kinematic viscosity, which is appropriately modified to include the effects of the other components.

The model for the concentration profile is based on the turbulent convective diffusion equation (Raudkivi, 1975), also appropriately averaged. The formulation entails modification of the eddy diffusivity to account for the presence of the solid particles and requires an accurate estimate of the solid vertical velocity component. This velocity is designated as a hypothetical solid vertical velocity. It is associated with an upward drag force, equivalent to the diffusion force, obtained from a force balance involving this force and terms representing the net gravitational, Coulombic, dispersive and lift forces. Our approach here differs from previous formulations (O'Brien, 1933; Roco and Balakrishnam, 1985; Roco and Mahadevan, 1986) in two important respects: we use a force balance which does include the lift force term, and we use the turbulent convective diffusion equation, as contrasted to Eq. 1, to calculate the concentration distribution. In addition, we use a new formulation for estimating the eddy diffusivity which enters the convective diffusion equation as shown later. This method allows us to calculate velocity and concentration profiles for each component, and, therefore, we are also able to calculate the holdup ratio.

The slurries considered in the present study are composed of a continuous liquid phase and $n - 1$ solid components. The solid components may have different densities and/or different average particle sizes. For a solid component with a broad particle size distribution, the solid phase may be subdivided into several narrow particle size components. In addition, the slurries are

noncolloidal and may be composed of fast settling and coarse particles.

The main underlying assumptions in the formulation of our slurry flow model are:

1. Both solid and liquid phases behave macroscopically as continua, but only the carrier fluid behaves microscopically as a continuum. This means that the volume-averaged equations are based on a control volume which is larger than the particle spacing but much smaller than the characteristic volume of the flow system.
2. The solid phase consists of spherical or at least isometrically shaped particles.
3. Neither the suspended solid nor the carrier fluid undergoes any phase changes.
4. There is no particle attrition.
5. Secondary flow is nonexistent or is negligible.

Governing equations for velocity profiles of components

The starting points for derivation of the equations for calculation of the velocity distributions of the various slurry components are the local volume-averaged continuity and momentum equations. Thus, in Cartesian tensor notation, the volume-averaged equation of continuity for component k is (Danon et al., 1977)

$$\frac{\partial}{\partial t}(C_k\rho_k) + \frac{\partial}{\partial x_j}(C_k\rho_k v_{kj}) = 0 \tag{2}$$

The momentum equations for component k (solid or liquid) are given by (Roco and Shook, 1983)

$$C_k\rho_k\frac{Dv_{ki}}{Dt} = C_k\rho_k g_i - C_k\frac{\partial P}{\partial x_i} - \frac{\partial}{\partial x_j}(C_k\tau_{kji}) - R_{kl_i} - R_{k(s-k)_i}, \quad (i = 1, 2, 3) \tag{3}$$

The terms R_{kl_i} and $R_{k(s-k)_i}$ designate the interactive forces, per unit volume of slurry, between component k and the liquid, and between component k and the remaining solid components, respectively. τ_{kji} is the ji-component of the stress tensor for slurry constituent k. As shown later, it consists of a viscous contribution due to the liquid phase and contributions due to solid-solid friction (Coulombic) for each solid component. The turbulent contributions to the stress reside in the convective terms of Eq. 3. The total number of slurry components, n, consists of $n-1$ solid components and one continuous liquid phase. Accordingly, we also have

$$\sum_{k=1}^{n} C_k = 1 \tag{4}$$

In these equations, k denotes the slurry component, $(s-k)$ denotes the solid content excluding component k, and the subscripts l and s designate liquid and solid phases, respectively.

The velocities, v_{kj}, and the concentrations, C_k, in the foregoing equations are the instantaneous values. The mean flow equations are obtained from these through conventional Reynolds averaging. For constant physical properties of all components, and macroscopically steady state (i.e., $\partial/\partial t = 0$) flow, the convective term in Eq. 3 may be expressed as

$$C_k\rho_k\frac{Dv_{ki}}{Dt} = \frac{\partial}{\partial x_j}[\rho_k\overline{C_k v_{kj}v_{ki}}] + \frac{\partial}{\partial x_j}[\rho_k\overline{C_k v'_{kj}v'_{ki}}] + \frac{\partial}{\partial x_j}[\rho_k\overline{v_{kj}C_k v'_{ki}}] + \frac{\partial}{\partial x_j}[\rho_k\overline{v_{ki}C'_k v'_{kj}}] + \frac{\partial}{\partial x_j}[\rho_k\overline{C'_k v'_{ki}v'_{kj}}] \tag{5}$$

In Eq. 5, the primes denote fluctuating components, and the overbars denote time-mean values. The overbars are not explicitly used when there is no likelihood for confusion between instantaneous, v_{ki}, and time-mean, $\bar{v}_{ki}$, quantities. Because the mean flow is assumed to be fully-developed, the only nonzero component of the mean velocity for all slurry components is the axial component, $\bar{v}_{kz}$, and thus also the first and third terms of the RHS of Eq. 5, which involve axial derivatives, are zero.

The Reynolds stresses in Eq. 5 are expressed using Boussinesq's (1877) hypothesis. Thus,

$$\rho_k\overline{v'_{ki}v'_{kj}} = \tau_{kij,t} = -\rho_k\left[\nu_{tk}\left(\frac{\partial\bar{v}_{ki}}{\partial x_j} + \frac{\partial\bar{v}_{kj}}{\partial x_i}\right) - \frac{2}{3}k\delta_{ij}\right] \tag{6}$$

where $k = (\overline{v_1'^2} + \overline{v_2'^2} + \overline{v_3'^2})/2$ vanishes for incompressible flow. By direct analogy with turbulent momentum transport, turbulent mass transport terms in Eq. 5 are assumed to have the form

$$\rho\overline{C'v'_j} = -\rho\epsilon_t\frac{\partial\bar{C}}{\partial x_j} \tag{7}$$

where $\epsilon_t = \nu_t/\sigma_t$ is the eddy diffusivity with σ_t equal to the turbulent Schmidt number.

To obtain the governing equation for calculation of velocity profiles we need to take the component of Eq. 2 in the axial direction, z, after the entire equation has been time-averaged. In the axial direction for this equation, the following terms are negligible: the diffusion terms arising from the convective term in Eq. 2, i.e., the last two terms in Eq. 5; the terms $\overline{C'dP'/dz}$ and $\partial\overline{C'\tau'_{jl}}/\partial x_j$; and the terms constituted of the fluctuating components in the interactive force terms (the R terms). As a result, Eq. 2 for the z direction reduces to

$$0 = -C_k\frac{dP}{dz} - \frac{\partial}{\partial x_j}(C_k\tau_{kjz,t}) - \frac{\partial}{\partial x_j}(C_k\tau_{kjz}) - R_{klz} - R_{k(s-k)z} \tag{8}$$

in which dependent variables are understood to be time-mean values. The term containing the turbulent stress, $\tau_{kjz,t}$, arises from the convective term, is in fact equivalent to the second term on the righthand side of Eq. 5, and is expressed in the form in Eq. 8 in consequence of our definition of the turbulent Reynolds stresses given by Eq. 6. The first, second and fourth terms in Eq. 8 are important in general, while the third term is important for $k = l$, and for $k \neq l$ in nonhomogeneous flow. The last term is important in situations in which there are large disparities in solid component velocities (e.g., when very large and very small particles or particles of different densities are present).

Our next task is to provide approximations for estimating the various terms in Eq. 8. These are the stresses (τ) and the interactive force (R) terms.

Stress terms, τ_{kjz} and $\tau_{kjz,t}$

As stated earlier the stress terms consist of the following contributions:

$$\tau_{kjz,\text{viscous}} = -\mu_k \frac{\partial v_{kz}}{\partial x_j}, \quad \text{for } k = l, \tag{9}$$

$$\tau_{kyz,\text{Coulombic}} = \sigma_{kyy} \tan \theta_d, \quad \text{for } k \neq l, \tag{10}$$

$$\tau_{kjz,t} = \tau_{kjz,\text{turbulent}} = -\rho_k \nu_{tk} \frac{\partial v_{kz}}{\partial x_j}, \quad \text{for all } k. \tag{11}$$

In Eq. 10, σ_{kyy} is the Coulombic normal stress for solid component k. It will be considered further in our discussion of the equation for calculating concentration profiles. The term $\tan \theta_d$ is the Coulombic dynamic friction coefficient. Its value depends on the solid material; for sand and glass beads it ranges from 0.45 to 0.65. Now an expression for estimating the eddy kinematic viscosity, ν_{tk}, in particle-laden flows is needed.

Eddy kinematic viscosity, ν_{tk}

The eddy kinematic viscosity reflects the apparent increase in kinematic viscosity due to turbulence. It can be calculated from knowledge of the shear stress and velocity distribution. According to Prandtl's (1925) mixing length model for single-phase flow, it is given by (assuming the proportionality constant to be unity)

$$\nu_t = l_m^2 \left| \frac{\partial u}{\partial y} \right| \tag{12}$$

In fully-developed duct flows the mixing length is given by Nikuradse's (1932) formula

$$\frac{l_m}{R} = 0.14 - 0.08\left(1 - \frac{y}{R}\right)^2 - 0.06\left(1 - \frac{y}{R}\right)^4 \tag{13}$$

where $y = R - r$ is the distance from the pipe wall. Equation 13 is valid for Reynolds numbers above 10^5 for rough as well as smooth walls. For Reynolds numbers below 10^5 we have, based on Nikuradse's data presented by Cebeci and Smith (1974), developed the following correction factor needed to multiply the righthand side of Eq. 13:

$$\psi_{corr} = 1 + \frac{0.12}{0.14} \exp\left[-0.0475\left(\frac{Re}{1{,}000} - 4\right)\right] \tag{14}$$

Furthermore, to account for turbulence damping close to the wall, the van Driest (1956) damping correction, given by

$$\psi_{damp} = \left[1 - \exp\left(-\frac{y v_*}{A\nu}\right)\right], \quad A = 26 \tag{15}$$

is used.

Eddy kinematic viscosity distributions measured by Nikuradse (1932), Laufer (1954) and by Nunner (1956) are in conflict; the different data lead to different empirical expressions. In view of this, we developed the expression

$$\nu_{to} = v_* R l_m [0.4(r/R)^2 + (0.6 - a)(r/R) + a] \psi_{corr} \psi_{damp} \tag{16}$$

in which the friction velocity $v_* = \langle v \rangle (f/2)^{1/2}$ is calculated from the resistance formula due to Colebrook and White (1937):

$$\frac{1}{f^{1/2}} = 3.48 - 4 \log_{10}\left[\frac{2S_k}{D} + \frac{18.7}{Ref^{1/2}}\right] \tag{17}$$

and the parameter a is given by

$$a = 1.7400 - 0.6705 \log (Re) + 0.0655 [\log (Re)]^2. \tag{18}$$

In Eq. 17, f is the Fanning friction factor and S_k is the absolute roughness of the pipe. We have tested Eq. 16 with data on water and it works very well.

The presence of solids further modifies the value of the kinematic viscosity. It is difficult to measure ν_{tk} for each slurry component, and no data are available. However, Pechenkin (1972) has observed, from experiments with relatively low concentrations of spherical solids, a decrease in measured eddy diffusivity; the decrease being approximately proportional to $(1 - C/C_{max})$, in which C_{max} is the maximum packing concentration. These experiments correspond to dilute, fully-suspended homogeneous flow effectively dominated by the continuous phase. Thus, for weak solid interactions we assume that

$$\frac{\tilde{\nu}_{tl}\rho_l}{\nu_{to}\rho_l} = \phi_l \simeq 1 - \frac{C_s}{C_{max}} \tag{19}$$

in which ν_{to} is the value in the absence of solids and C_s is the total solids concentration. Roco and Balakrishnam (1985) have used Eq. 19, assuming it to be valid for all solids concentrations. We view the presence of solids, under conditions of high concentration, to have a stronger dampening effect on the liquid eddy viscosity.

Equation 19 is for the continuous phase. For the solid components, since we can assume that interparticle interaction increases in inverse proportion to relative spacing between particles, and that sedimentation is retarded by increased particle interaction, we take the eddy kinematic viscosity for the solid component to be given by

$$\frac{\tilde{\nu}_{tk}\rho_k}{\nu_{to}\rho_l} = \phi_k \simeq \frac{(1 - C_s)^c \exp\left(\dfrac{2C_k}{Fr_k^{1.5}}\right)}{\left(1 - b\dfrac{C_s}{C_{max}}\right)^{a_k}}, \quad k \neq l \tag{20}$$

with

$$c = 1 + Fr_k[\langle C_{ins} \rangle - 0.5 C_{max}] \geq 1 \tag{21}$$

The empirical coefficient a_k is equal to 1.5, and b is 1 or 1.25 according to whether ϕ_k is used to estimate the eddy kinematic

viscosity or the eddy diffusivity, respectively. The factor c is used to account for the severe damping of the turbulence at very high solids concentration. In analogy to the definition by Shield (1936), the modified Froude number, Fr_k, in Eq. 20 is defined by

$$Fr_k = \frac{v_*^2}{gd_k(s_k - s_{m-k})} \tag{22}$$

where $s_k = \rho_k/\rho_l$. The tildes in Eqs. 19 and 20 are used to emphasize that these relationships are restricted to conditions of relatively weak interactions among the various components of the slurry. We note here that, unlike previous workers (e.g., Roco and Shook, 1983, 1985; Roco and Mahadevan, 1986), our Froude number definition given by Eq. 22 is component-specific.

To include stronger component interactions within the framework of a uniformly valid formulation, and thereby to relax the foregoing restriction, we take

$$\frac{\nu_{tk}\rho_k}{\nu_{to}\rho_l} = \Phi_k = \phi_k + \alpha C_k(\phi_{m-k} - \phi_k) \geq s_m, \quad \text{for all } k \tag{23}$$

with

$$\phi_{m-k} = \sum_{h \neq k} C_h\phi_h/(1 - C_k) \tag{24}$$

In Eq. 23, α has a value of about 0.75 and s_m is the local density ratio of mixture to carrier fluid.

Interactive force term, R_{kli}

Our formulation for the interactive force, R_{kli}, between solid component k and the liquid starts with consideration of the drag force on a single particle. This is then modified to include the effects of other particles. For a solitary particle of solid component k the drag force is given in terms of the single particle drag coefficient by

$$F_{D_{ko}} = C_{D_{ko}}\rho_l \frac{\pi d_k^2}{4} \frac{(v_k - v_l)|v_k - v_l|}{2} \tag{25}$$

For N_k particles of solid component k with concentration C_k, the total drag force per unit volume due to viscous effects may be estimated by Brinkman's (1947) model, which pertains to viscous flow through a swarm of spherical particles. This drag force is given by

$$F_{D_{kN}} = N_k F_{D_{ko}}\left(1 + \frac{d_k}{2\sqrt{\kappa_k}} + \frac{d_k^2}{12\kappa_k}\right) \tag{26}$$

in which the permeability κ_k may be estimated from

$$\kappa_k = \frac{d_k^2}{72}\left[3 + \frac{4}{C_k} - 3\left(\frac{8}{C_k} - 3\right)^{0.5}\right] \tag{27}$$

Equation 26 is applicable to dilute as well as concentrated suspensions (Happel and Brenner, 1983). Accordingly,

$$R_{kl_i} = N_k F_{D_{ko}}\left[1 + \frac{d_k}{2\sqrt{\kappa_k}} + \frac{d_k^2}{12\kappa_k}\right] \tag{28}$$

in which $N_k = 6C_k/(\pi d_k^3)$. Equation 28 gives the net interactive force between solid component k and the liquid. The net interactive force between liquid and the total solid phase is then the sum of all the individual forces for each solid component.

Interactive force term, $F_{k(s-k)i}$

The interactive force per unit volume among particles of the same solid component is defined as the x_i derivative of the Coulombic frictional stress given by Eq. 10. It results from collisions due to the fluctuating motions of the particles and friction between solid layers. In addition to these two effects, however, the interactive force between two different solid components must additionally account for interactive force enhancement arising from the difference in solid velocities at the same position. The former effects are again accounted for by the derivative of the appropriate Coulombic stress. The effect arising from the difference in local velocities of the different solid components is considered here.

First consider solid component k and h. For each the force associated with the axial direction is the derivative of the shear stress. The net interactive force between the two components is then the difference between the two forces multiplied by the probability of contact between the two kinds of particles. We take the probability of contact to be C_hC_k, and therefore

$$R_{kh_i} = C_kC_h \frac{\partial}{\partial x_j}\left(\rho_k\nu_{tk}\frac{\partial v_{ki}}{\partial x_j} - \rho_h\nu_{th}\frac{\partial v_{hi}}{\partial x_j}\right) \tag{29}$$

Then the resultant interactive force between solid component k and the remaining solid components is given by the sum

$$R_{k(s-k)_i} = \sum_{\substack{h=1 \\ h \neq k}}^{n} R_{kh_i} \tag{30}$$

Boundary conditions on velocities

The no-slip condition is enforced at the pipe wall for both solid and liquid components. In addition the mixture velocity is required to obey the relationship

$$\int_A v_m\, dA = \langle v_m \rangle_{dis} A \tag{31}$$

The enforcement of this constraint serves both as a check on velocity profile calculations and also as an extra equation for determining the extra unknown, the pressure drop $(-dp/dz)$.

Governing equations for concentration profiles

The basic mechanism underlying the model for calculation of the concentration profiles rests on the presumption of a dynamic balance between particle settling and particle dispersion in consequence of the random motion inherent to the flow. The process is modeled by appropriately adapting the generalized diffusion

equation, with the convective terms modified to represent particle settling and the diffusive terms to represent particle dispersion. The starting point is the equation

$$\frac{\partial C}{\partial t} + v_i \frac{\partial C}{\partial x_i} = \epsilon_m \frac{\partial^2 C}{\partial x_i \partial x_i} \tag{32}$$

Reynolds averaging of Eq. 32 for steady turbulent flow gives

$$v_i \frac{\partial C}{\partial x_i} = \frac{\partial}{\partial x_i}\left(\epsilon_{ij} \frac{\partial C}{\partial x_j} + \epsilon_m \frac{\partial C}{\partial x_i}\right) \tag{33}$$

in which ϵ_m refers to molecular diffusion, and ϵ_{ij} is the turbulent eddy diffusivity tensor. All dependent variables in Eq. 33 are time-mean values. In turbulent flow the components of ϵ_{ij} are much larger than ϵ_m, and the latter may be neglected. Further, since there is no evidence that significant variation of transverse velocity with direction exists, it is assumed that the diffusion is isotropic. Accordingly, ϵ_{ij} is henceforth replaced by ϵ_t (Yuu, 1985). The eddy diffusivity, ϵ_t, is a function of suspension flow properties as well as the flow conditions.

The convective term on the LHS of Eq. 33 represents the effects of particle settling and only has a vertical component. Particle settling is a function of solids concentration, as manifested in the hindered settling effect in gravity sedimentation, but in slurry transport it is also dependent on the turbulent flow and effects associated with, for example, the dispersive force, the shear-slip effect and the Coulombic contact force. Strictly, at steady state the actual mean vertical velocity for all slurry components, v_{ky}, is zero. Accordingly, the solid vertical velocity component to be used in Eq. 33 is a hypothetical velocity designated by $\tilde{v}_{ky}$; it is designed to account for the settling effects on particle transport. For steady state, fully-developed flow Eq. 33 for solid component k thus becomes

$$\tilde{v}_{ky} \frac{\partial C_k}{\partial y} + \frac{\partial}{\partial x}\left(\epsilon_t \frac{\partial C_k}{\partial x}\right) + \frac{\partial}{\partial y}\left(\epsilon_t \frac{\partial C_k}{\partial y}\right) = 0 \tag{34}$$

Equation 34, together with appropriate boundary conditions and constraints, provide the basic computational form for estimation of the concentration profile. Appropriate formulations for $\tilde{v}_{ky}$ and ϵ_t are needed.

To establish the relationship for estimating the hypothetical vertical velocity, $\tilde{v}_{ky}$, we make use of the equation of motion, taken in the direction of the gravitational force, $-y$. In the y-direction the time-mean velocities for all slurry components (solid and liquid) $v_{ky} = 0$, and the equation of motion becomes

$$\frac{\partial}{\partial x_j}[\rho_k C_k \overline{v'_{ky} v'_{kj}}] + \frac{\partial}{\partial x_j}[\rho_k \overline{C'_k v'_{ky} v'_{kj}}] = C_k \rho_k g - C_k \frac{\partial P}{\partial y} - \overline{C'_k \frac{\partial P'}{\partial y}} - \frac{\partial}{\partial x_j}(C_k \tau_{kjy}) - \frac{\partial}{\partial x_j}\overline{C'_k \tau'_{kjy}} - \overline{R'_{kly}} - \overline{R'_{k(s-k)y}}. \tag{35}$$

The net forces which determine the hypothetical vertical velocity for solid component k are measured against the forces associated with the liquid displaced by solid k as a reference. The latter reference forces are given by the product of the ratio (C_k/C_l) with Eq. 35 for $k = l$. When the resulting equation is subtracted from Eq. 35, we obtain the desired equation for these net forces. This equation may be viewed as a balance among five major force terms, given as

$$\underbrace{\left\{\frac{\partial}{\partial x_j}[\rho_k C_k \overline{v'_{ky} v'_{kj}}] + \frac{\partial}{\partial x_j}[\rho_k \overline{C'_k v'_{ky} v'_{kj}}]\right\} - \frac{C_k}{C_l}\left\{\frac{\partial}{\partial x_j}[\rho_l C_l \overline{v'_{ly} v'_{lj}}] + \frac{\partial}{\partial x_j}[\rho_l \overline{C'_l v'_{ly} v'_{lj}}]\right\}}_{F_{diff}}$$

$$= \underbrace{\overline{C'_k \frac{\partial P'}{\partial y}} + \frac{C_k}{C_l}\overline{C'_l \frac{\partial P'}{\partial y}}}_{F_{diff}} + \underbrace{C_k(\rho_k - \rho_l)g}_{F_{grav}} - \underbrace{\frac{\partial}{\partial x_j}(C_k \tau_{kjy})}_{F_{Coul}} + \underbrace{\frac{C_k}{C_l}\frac{\partial}{\partial x_j}(C_l \tau_{ljy})}_{=0}$$

$$\cdot \underbrace{\frac{\partial}{\partial x_j}\overline{C'_k \tau'_{kjy}} + \frac{C_k}{C_l}\frac{\partial}{\partial x_j}\overline{C'_l \tau'_{ljy}} - \overline{R'_{k(s-k)y}}}_{F_{disp}} - \underbrace{\overline{R'_{kly}}}_{F_{lift}} \tag{36}$$

The forces F_{diff}, F_{grav}, F_{Coul}, F_{disp} and F_{lift} are the turbulent diffusion term, the buoyed gravitational force term, the Coulombic normal force term, Bagnold's dispersive force term and Saffman's lift force term, respectively. In Eq. 36, F_{diff}, F_{grav}, and F_{disp} are important in most situations. The magnitude of F_{Coul} increases with increase in the local concentration, and is sensitive to the shape of the concentration profile: i.e., it is quite sensitive to the nature of the flow regime which prevails. F_{lift} is important in the wall region, and is an order of magnitude smaller than the other terms in the center of the pipe. Equation 36 will be used to estimate $\tilde{v}_{ky}$. Except for F_{grav} the expressions for estimating the terms in Eq. 36, and their derivation, are rather complicated.

Turbulent diffusion term, F_{diff}

This term is difficult to derive as a force term. Its value is, therefore, calculated using Eq. 36 when the values of all other terms are determined as shown below. Our main hypothesis was that the forces inherent to turbulent diffusion were responsible for maintaining solid suspension. Accordingly, we take F_{diff} to be expressible as an upward turbulent drag force pertaining to the cloud of particles, and given by

$$F_{diff} = F_{drag} = N_k \rho_l \tilde{C}_{Dk} \frac{\pi d_k^2}{4} \frac{\tilde{v}_{ky}^2}{2} \tag{37}$$

in which N_k is the number of particles of component k per unit volume, and $\tilde{C}_{Dk}$ is the drag coefficient in terms of $\tilde{v}_{ky}$.

Our definition of the drag force, given by Eq. 37, differs from that used by Roco and coworkers (Roco and Shook, 1983, 1985; Roco and Balakrishnam, 1985). They use the form

$$F_{drag} = N_k \rho_l C_{Ds} \frac{\pi d_k^2}{4} \frac{\omega^2}{2} \tag{38}$$

in which, as stated earlier, the settling velocity ω is given in

terms of concentration according to Eq. 1. However, the drag coefficient $C_{Ds} = [(4/3)d(s-1)g]/\omega_s^2$ is defined in terms of the hindered settling velocity, ω_s, calculated according to Richardson and Zaki's (1954) equation

$$\omega_s = \omega_o(1-C)^n \tag{39}$$

where ω_o is the settling velocity of a single particle and n is the Richardson-Zaki coefficient.

With F_{diff} known, Eq. 37 is used to estimate $\tilde{v}_{ky}$ provided the drag coefficient $\tilde{C}_{Dk}$ is known. We use the drag coefficient correlation of Turian and Yuan (1977) to determine $\tilde{C}_{Dk}$ and $\tilde{v}_{ky}$. These equations are

$$\begin{aligned}\log_{10}Re_k = &-1.38 + 1.94\log_{10}\Lambda \\ &-8.60\times10^{-2}(\log_{10}\Lambda)^2 \\ &-2.52\times10^{-2}(\log_{10}\Lambda)^3 \\ &+9.19\times10^{-4}(\log_{10}\Lambda)^4 \\ &+5.35\times10^{-4}(\log_{10}\Lambda)^5\end{aligned} \tag{40}$$

with

$$\Lambda = Re_k\tilde{C}_{Dk}^{1/2} = \left[\frac{4}{3}\frac{gd_k^3\rho_l(\rho_k-\rho_l)}{\mu_l^2}\right]^{1/2} \tag{41}$$

$$Re_k = \rho_k\tilde{v}_{ky}d_k/\mu_l \tag{42}$$

Coulombic force term, F_{Coul}

For highly loaded slurry flows, the cloud of particles may not be solely suspended by the turbulent force. A part of the weight of the particles is supported by the inferior layer of solid particles or the pipe wall. This supporting force is referred to as the Coulombic normal force and is modeled, in accordance with Roco and Shook (1983), by

$$F_{Coul} = \frac{\partial}{\partial y}\sigma_{k,sl_{yy}} \tag{43}$$

where

$$\begin{aligned}\sigma_{k,sl_{yy}} &= \text{Coulombic normal stress for component } k \\ &= \int_y^D \lambda(y)(\rho_k - \rho_{m-k})gC_k\,dy\end{aligned} \tag{44}$$

$$\begin{aligned}\lambda(y) &= \text{coefficient of the support load} \\ &= (C_{sl}/Fr_k)^{E_{sl}}\end{aligned} \tag{45}$$

E_{sl}, C_{sl} are empirical constants which have values of about 2.0 and 0.25, respectively.

Bagnold's dispersive force term, F_{disp}

Bagnold (1954) obtained the relationship between shear stress and normal dispersive stress as

$$\tau_{disp} = \tau_{xy}/\tan\theta \tag{46}$$

For a slurry flow with multiple solid components, the enhancement in dispersive force may be approximated by

$$F_{k,disp} = \frac{\partial}{\partial y}\left(\frac{\tau_{k_{xy,turb}}}{\tan\theta}\right) - \frac{R_{k(s-k)_x}}{\tan\theta} \tag{47}$$

Here $\tan\theta = \beta C_{max}$ is the Bagnold coefficient, in which β is an empirical coefficient having values ranging from 0.55 to 0.65 depending on the material of the particles.

Saffman's lift force term, F_{lift}

Saffman's (1965) obtained the net force acting on a small translating sphere that was simultaneously rotating in an unbounded, uniform, simple shear flow field, the translation velocity being parallel to the streamlines of the fluid. It is shown that a particle of component k experiences a transverse lift force due to a shear-slip effect, given by

$$F_{lift} = 6.46N_k\mu_1\frac{d_k^2}{4}\frac{v_{kz}-v_{lz}}{\nu_l^{1/2}}\left|\frac{dv_{lz}}{dy}\right|^{1/2} \tag{48}$$

Rubin's (1977) experimental work confirmed Saffman's (1965) theoretical prediction for the lift force due to the shear-slip effect. The most surprising result was that, although Eq. 48 was derived for an unbounded ambient fluid flow, the agreement with experiment seems to persist even in the worst possible case in which the sphere is practically touching the wall. Therefore, the lift force on particles due to the shear-slip effect as predicted by Saffman's theory is used in the slurry flow model. The foregoing expressions for the various force terms in Eq. 36 permit us to estimate $\tilde{v}_{ky}$, through Eq. 37, for use in determining the concentration distribution from Eq. 34. We also need to estimate the eddy diffusivity, ϵ_t, in Eq. 34.

Eddy diffusivity, ϵ_t

For a highly loaded slurry, the eddy diffusivity is affected by the presence of all components. In the present study, therefore, the eddy diffusivity distribution is modeled by the relation

$$\epsilon_t = \frac{\nu_{lo}}{\sigma_{tm}}\left[\sum_h^n (C_hs_h\phi_h)^2\right]^{1/2} \tag{49}$$

where σ_{tm} is the turbulent Schmidt number for the mixture. Because the turbulent Schmidt number is an average value for the pipe cross-section, it is a function of the average *in situ* concentration, $\langle C\rangle_{ins}$. Furthermore, it is a function of the modified Froude number, Fr_s, based on d_{50}, and the average density for all solid components. Tests we have carried out suggest that σ_{tm} may be expressed as

$$\sigma_{tm} = \frac{1.0}{(1-\langle C\rangle_{ins})^{\xi}\exp(1/Fr_s)} \tag{50}$$

with

$$\xi = 1.25 + Fr_s^{1.75}[\langle C_{ins}\rangle - 0.5C_{max}] \tag{51}$$

where Fr_s has a value greater than 0.4 and ξ has a value ranging from 1.25 to 4.7. In addition, the ϕ_k for the solid components have the same form as in Eq. 20, but in this case with b taken as

1.25 in order to represent the maximum packing concentration associated with the gravitational sedimentation.

Boundary conditions for concentration profiles

The boundary conditions for the concentration equations state that at a solid wall, the mass flux will be equal to zero:

$$C(\vec{n} \cdot \tilde{v}_{ky}) + \epsilon_t \frac{\partial C}{\partial \vec{n}} = 0 \tag{52}$$

In addition, as with the case for the velocity profiles, we require that

$$\int_A (C_k v_m)\, dA = \langle C_k \rangle_{dis} \langle v_m \rangle_{dis} A \tag{53}$$

Aside from providing a test for the calculated concentration profile, the constraint specified in Eq. 53 provides a means for adjusting the assumed concentration at the bottom of the pipe in the numerical iteration scheme.

Computational Method

The governing equations for the velocity and concentration profiles, Eqs. 8 and 34, are coupled elliptic partial differential equations. The numerical code for solving these equations consisted of applying Galerkin's method and solving the resulting system using finite elements. Because of symmetry relative to the central vertical plane, only half the cross-sectional domain is considered and is discretized using 12 × 23 isoparametric quadrilateral elements. In view of the steepness of the velocity gradient in the wall region, a denser mesh is used in this region. Iterative procedures were used to solve the equations for velocity and concentration separately. The detailed derivation of the slurry flow model, and the description of the computational method including a listing of the numerical code are given by Hsu (1987).

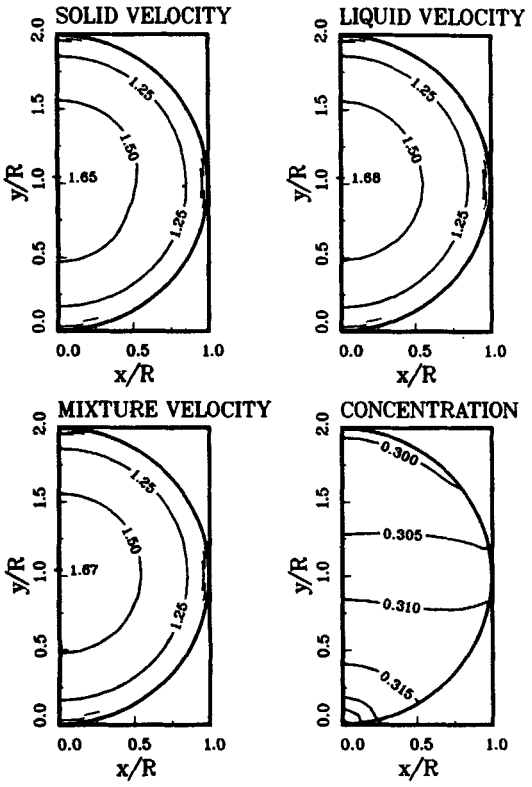

Figure 1. Contours of velocity and concentration distributions for 38.3 μm gypsum slurry in 5.263 cm pipeline: Run GP4.

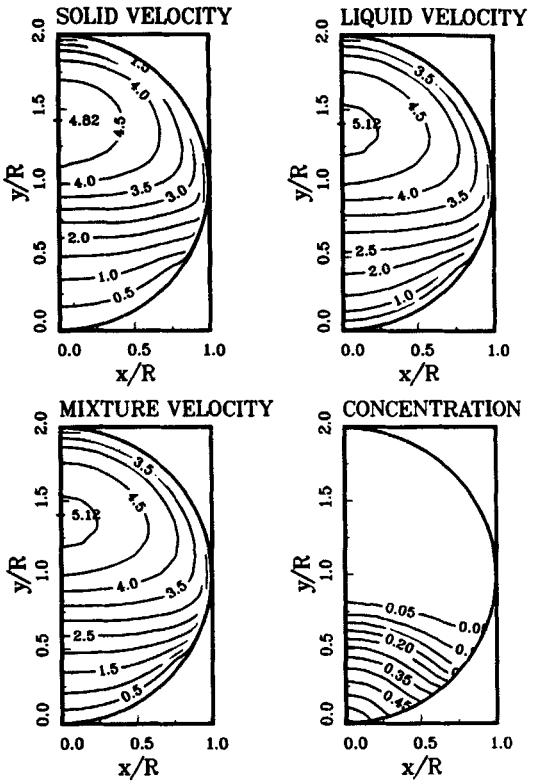

Figure 2. Contours of velocity and concentration distributions for 13,000 μm gravel slurry in 26.3 cm pipeline: Run GR1.

Applications of Model and Experimental Verification

Calculations based on the slurry flow model and comparisons with experiment were carried out for single-phase flow (as part

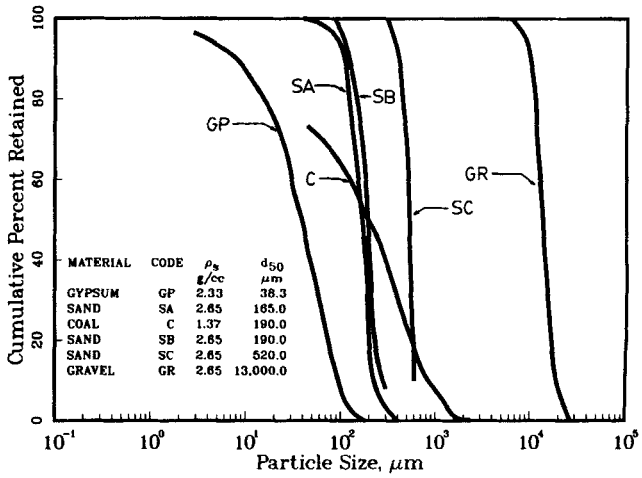

Figure 3. Particle size distributions for test solids.

Table 1. Comparison of Slurry Model Calculations, Rheologically-Based Correlation Predictions, and Experimental Data*

No.	$\langle C \rangle_{dis}$ Exp.	$\langle C \rangle_{dis}$ Cal.	Holdup Ratio	$\langle v_m \rangle$ m/s Exp.	$\langle v_m \rangle$ m/s Cal.	$(-dP/dz)$ Pa/m Exp.	$(-dP/dz)$ Pa/m Cal.	$(-dP/dz)$ Pa/m Rheol.**
GP1	0.107	0.107	1.0009	1.11	1.11	294.1	294.0	287.6
GP2	0.107	0.106	1.0000	3.01	3.00	1,651.3	1,696.0	1,647.9
GP3	0.107	0.107	1.0000	4.81	4.80	3,822.9	3,946.0	3,742.8
GP4	0.306	0.308	1.0003	1.33	1.33	542.9	542.9	576.3
GP5	0.306	0.306	1.0000	3.12	3.11	2,352.6	2,271.0	2,562.5
GP6	0.306	0.306	1.0000	4.70	4.69	4,727.7	4,706.0	5,248.8

*Gypsum slurries in 5.263 cm pipe
**Calculated values by Ma's (1987) rheologically-based model

of tests of the model in the dilute limit), and for slurries comprised of seven different particle sizes covering five solids. The calculations for the slurry flows included determination of detailed component and mixture velocity and concentration distributions (e.g., Figures 1 and 2), as well as pressure gradients and holdup ratios. The test slurries (and slurry code and median particle size) chosen for these calculations and tests against experiment were: gypsum (GP, 38.3 μm), sand (SA, 165.0 μm), coal (C, 190.0 μm), sand (SB, 190.0 μm), sand (SC, 520.0 μm), glass (GL, 580.0 μm), and gravel (GR, 13,000 μm). The particle size distribution data for all these solids, except for the 580.0 μm glass slurries, are given together with solid density data in Figure 3. It is evident that, except for gypsum and coal, the size distributions are rather narrow. Size distribution data for the glass particles were not reported (Scarlett and Grimley, 1974). These test slurries were chosen because detailed experimental data, including velocity and concentration distribution data were available (Schriek et al., 1973; Scarlett and Grimley, 1974; Roco and Shook, 1982, 1983; Shook et al., 1982; Gillies et al., 1983; and the present work). Altogether 44 cases of slurry flow

Table 2. Comparison of Model Calculation for Pressure Drop with Experimental Data for Coal, Sand, and Gravel Slurries in Pipeline of Various Diameters

No.	D m	$\langle C \rangle_{dis}$ Exp.	$\langle C \rangle_{dis}$ Cal.	Holdup Ratio	$\langle v_m \rangle$ m/s Exp.	$\langle v_m \rangle$ m/s Cal.	$(-dP/dz)$ Pa/m Exp.	$(-dP/dz)$ Pa/m Cal.	Temp. °C
C1	0.2085	0.326	0.323	1.0019	2.59	2.59	266.5	281.0	20
C2	0.2085	0.327	0.329	1.0030	2.34	2.34	226.3	239.0	20
C3	0.2085	0.333	0.335	1.0069	2.01	2.01	177.3	187.0	20
C4	0.2085	0.327	0.328	1.0299	1.78	1.78	147.0	152.0	20
C5	0.2085	0.323	0.321	1.0482	1.59	1.58	123.4	126.0	20
C6	0.2085	0.327	0.329	1.0635	1.37	1.37	99.9	104.0	20
SA1	0.0515	0.084	0.084	1.133	1.66	1.66	666.2	668.9	20
SA2	0.0515	0.092	0.092	1.026	3.78	3.77	2,449.2	2,590.0	20
SA3	0.0515	0.187	0.188	1.104	1.66	1.66	901.3	878.2	20
SA4	0.0515	0.189	0.189	1.002	4.17	4.17	3,428.9	3,423.0	20
SA5	0.0515	0.280	0.279	1.049	1.66	1.66	1,136.4	1,141.0	20
SA6	0.0515	0.286	0.285	1.000	4.33	4.32	4,408.1	4,309.0	20
SA7	0.2630	0.103	0.104	1.105	2.90	2.89	261.6	265.4	20
SA8	0.2630	0.100	0.100	1.086	3.50	3.50	334.1	358.0	20
SA9	0.2630	0.190	0.191	1.080	2.90	2.89	305.7	306.4	20
SA10	0.2630	0.184	0.183	1.066	3.50	3.49	382.1	398.9	20
SA11	0.2630	0.270	0.272	1.044	2.90	2.91	355.6	356.2	20
SA12	0.2630	0.268	0.269	1.032	3.50	3.49	453.6	454.0	20
SA13	0.2630	0.341	0.343	1.036	2.90	2.89	414.4	409.0	20
SA14	0.2630	0.338	0.339	1.043	3.50	3.51	526.1	503.8	20
SA15	0.4950	0.104	0.104	1.103	3.16	3.15	143.0	146.0	20
SA16	0.4950	0.100	0.101	1.083	3.76	3.75	186.1	193.0	20
SA17	0.4950	0.187	0.188	1.083	3.07	3.06	157.7	164.9	20
SA18	0.4950	0.184	0.185	1.066	3.76	3.75	210.6	219.7	20
SA19	0.4950	0.273	0.272	1.043	3.16	3.15	193.0	200.9	20
SA20	0.4950	0.269	0.270	1.034	3.76	3.75	254.7	250.0	20
SB1	0.1585	0.150	0.151	1.099	2.50	2.49	475.2	470.0	10
SB2	0.1585	0.300	0.301	1.035	2.50	2.50	630.9	628.9	10
SB3	0.1585	0.150	0.151	1.184	3.00	2.99	648.9	667.1	60
SB4	0.1585	0.300	0.301	1.081	2.90	2.89	866.7	879.1	60
SC1	0.0507	0.1212	0.1217	1.310	1.90	1.90	1,175.6	1,215.0	20
SC2	0.0507	0.2473	0.2484	1.202	2.00	2.00	1,763.4	1,701.0	20
GR1	0.2630	0.090	0.091	2.420	3.20	3.20	842.5	781.8	20
GR2	0.2630	0.090	0.091	2.045	4.00	3.99	989.5	1,053.0	20

Table 3. Comparison of Model Calculations for Mean Liquid and Solid Velocities with Experimental Data for Crushed Glass Slurries*

No.	$\langle C \rangle_{dis}$ Exp.	$\langle C \rangle_{dis}$ Cal.	Holdup Ratio	$\langle v_m \rangle$ m/s Exp.	$\langle v_m \rangle$ m/s Cal.	$\langle v_l \rangle$ m/s Exp.	$\langle v_l \rangle$ m/s Cal.	$\langle v_s \rangle$ m/s Exp.	$\langle v_s \rangle$ m/s Cal.
GL1	0.170	0.170	1.056	2.88	2.88	2.91	2.92	2.68	2.70
GL2	0.160	0.160	1.133	2.70	2.70	2.74	2.77	2.50	2.36
GL3	0.120	0.120	1.177	2.01	2.01	2.03	2.05	1.77	1.69
GL4	0.080	0.081	1.307	1.05	1.05	1.12	1.07	0.79	0.79

*in 4.0 cm pipe

as listed in Tables 1 through 3 were considered. For each case, in addition to pressure gradient and holdup ratio, velocity and concentration distribution contour curves were calculated. Because of page constraints, only two cases are shown here, Figures 1 and 2; the remaining plots are given by Hsu (1987), which also contains plots comparing calculated and experimental velocity and concentration distributions such as those in Figures 4, 5 and 6. A summary of the results of the numerical simulations based on our slurry flow model and the comparisons with experiment is:

Single-phase flow

Pressure gradient calculations for single-phase flow for the Reynolds number range relevant to slurry flows, $Re = 2.3 \times 10^4$ to 3.2×10^6, were compared to those calculated using Blasius's (for $Re < 10^5$) and Prandtl's (for $Re > 10^5$) resistance formulae. The differences were within 1%. Furthermore, comparisons of detailed single-phase velocity distributions calculated using our

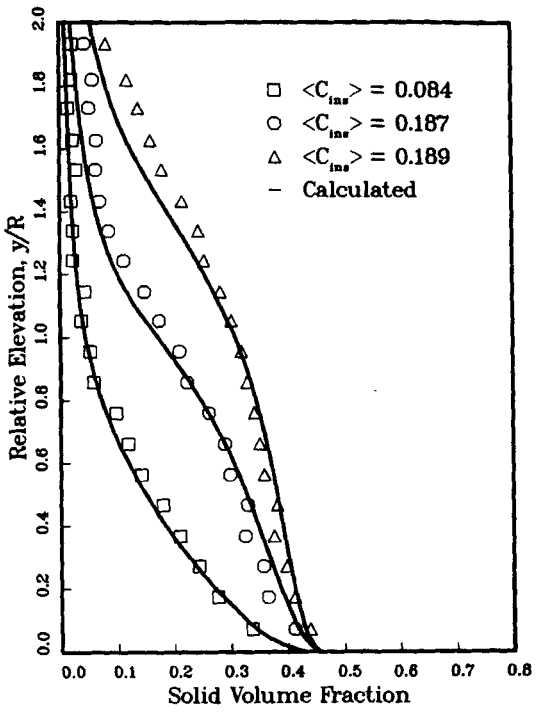

Figure 4. Vertical profiles of chord-averaged solids concentration of sand slurries pipeline: Runs SA1, SA3 and SA5.
Experimental data are extracted from Roco and Shook (1982).

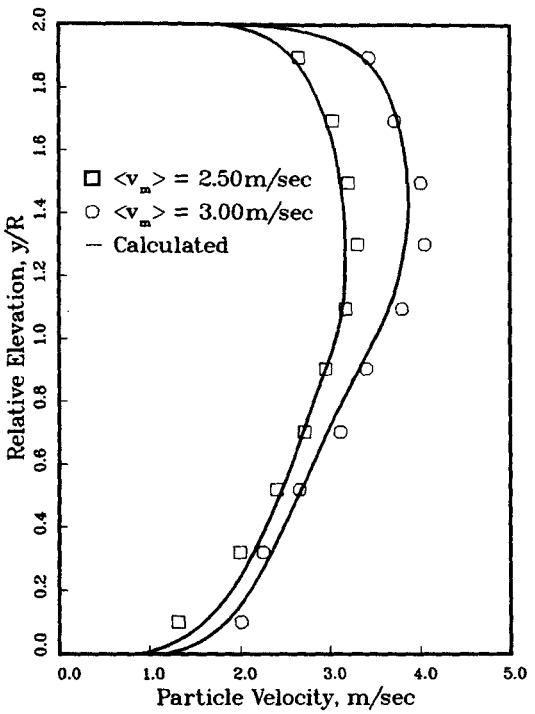

Figure 5. Particle velocity profiles along vertical axis of pipe for 190 μm sand slurry in 15.85 cm pipeline: Runs SB1 (T = 10°C) and SB3 (T = 60°C).
Experimental data are extracted from Gillies et al. (1983).

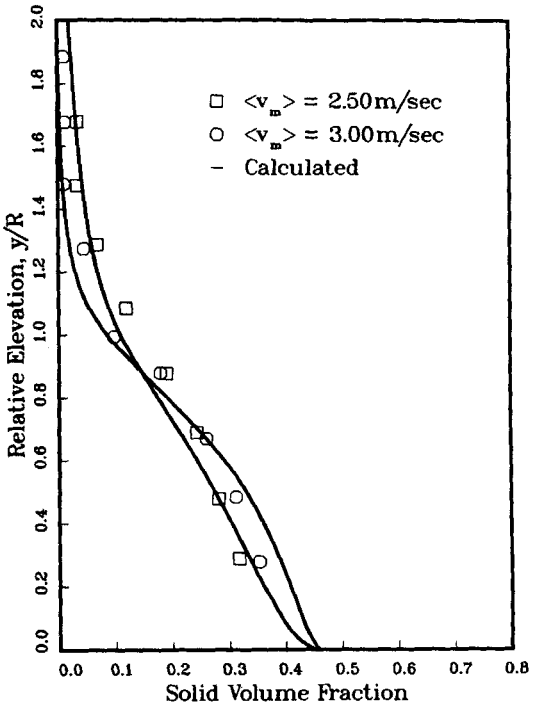

Figure 6. Vertical profiles of chord-averaged solids concentration for 190 μm sand slurry in 15.85 cm pipeline: Runs SB1 (T = 10°C) and SB3 (T = 60°C).
Experimental data are extracted from Gillies et al. (1983).

model with the experimental data of Nikuradse (1932) resulted in excellent agreement. It should be noted that the solids concentration limits of our slurry flow model extend from single-phase flow to virtually near 70% of maximum packing.

Comparisons of continuum rheological approach with present model

The test cases for the gypsum slurry listed in Table 1 provide an opportunity to compare the following two approaches for prediction of slurry pressure drops: the rheologically-based, continuum approach appropriate to fine particulate slurries which settle sufficiently slowly to permit meaningful rheological measurements and the present multiphase flow model approach. Measurements on gypsum slurries were carried out in a companion study in our laboratory concerned with the flow of concentrated, fine particulate, non-Newtonian slurries (Ma, 1987). In this work it was found that the shear stress/shear rate dependence of the gypsum slurries followed the Sisko model, and consequently model-specific friction loss correlations for laminar and turbulent pipeline flow were developed by Ma (1987). Table 1 lists the comparison of pressure gradients calculated using the present multiphase flow model and also the rheologically-based friction loss correlation with the measured values. These results are significant because: the present model evidently does an excellent job of predicting pressure losses for even very fine particulate slurries, and, moreover, provides *in situ* velocity and concentration distributions, Figure 1; for fine particulate slurries, the continuum rheological approach represents a feasible method for correlating friction loss data and may well be inevitable for submicron particle suspensions for which colloidal effects are dominant. In brief, the gypsum slurries, containing particles from about 10–80 μm, represent an overlap system bridging the two approaches.

Solids concentration effects

The concentration distributions are more uniform for higher average concentrations at the same average velocity as shown for sand slurries in Figure 4. Consequently, the velocity distribution is less asymmetric across the vertical plane. Because the experimental concentration profiles were obtained using gamma-ray absorption, the concentration profiles shown in Figure 4 correspond to chord-averaged values. Furthermore, the holdup ratio defined by

$$\text{holdup ratio} = \frac{\langle C\rangle_{ins}}{\langle C\rangle_{dis}} = \frac{\int_A C\,dA}{\int_A [v_m/\langle v_m\rangle] C\,dA} \tag{54}$$

decreases with increasing average concentration, as shown in Table 2. This apparently surprising finding results from the fact that, at a given mean mixture velocity, the concentration gradient is less steep for the higher average concentration, and consequently the mixture velocity distribution is less asymmetric across the vertical plane. The contribution to the integrand $[Cv_m/\langle v_m\rangle]$ in Eq. 54 from the middle and upper regions of the pipe cross-section, where $v_m/\langle v_m\rangle$ is larger, is relatively smaller for the case of a lower average concentration because the local value of C is low. Consequently, the holdup is higher. Moreover, the local concentrations in the lower part of the pipe cross-section are about the same for both low and high average concentrations, and therefore the contribution to the integrand from this region of the pipe cross-section further tends to depress the value of the integral in the case of the lower average concentration. It should be noted, however, that as the average solids concentration increases to very high values the resulting severe damping of the turbulence may lead to reduction in particle transport and therefore a reversal in the trend.

Particle size effects

Particle sizes have two main effects on slurry flow behavior. Increasing the particle size leads to: 1. an increase in the Coulombic normal force, and consequently an increase in the pressure gradient and the slip velocity; and 2. an increase in the gravitational force, and consequently a steepening of the concentration gradient in the vertical direction. Contour plots for flow of 13,000 μm gravel slurries shown in Figure 2 demonstrate these effects. Close examination of Tables 1–3 would lead to the same conclusions.

Density ratio effects

According to the model, it is known that increasing the density ratio results in effects similar to increasing the particle size. However, it is suspected that factor the a_k in Eq. 20 may be a function of the terminal velocity of the solid particles. The parameter a_k is taken to have a value of 1.5 which corresponds to particles having a specific gravity of about 2.3, such as sand and glass beads. However, the density of coal is only about half of the density of the other materials examined in the present work. It is evident that without adjusting the value of a_k pressure gradient deviations of about 6% result, as shown in Table 2.

Temperature effects

Cases SB1–SB4 permit us to assess the effect of temperature. Because the change in fluid density is about 2%, while the change in the fluid viscosity is about tenfold when the temperature changes from 60°C to 10°C, this also provides an assessment of the effect of fluid viscosity. The comparisons of the calculated and the experimental solid velocity profiles along the vertical central plane are given in Figure 5. The comparisons of calculated and experimental chord-averaged concentrations are given in Figure 6. It is observed that although the velocities are higher for the 60°C flows, the local concentrations are higher in the lower section and lower in the upper section of the pipe than for the flows at 10°C. Furthermore, the holdup ratios for tests SB1 and SB2 are less than those for SB3 and SB4, respectively, in spite of the higher velocities in the latter cases, as shown in Table 2. These are clearly due to the effect of viscosity. Decreasing the viscosity results in a decrease in the friction velocity, and consequently in the modified Froude number. Accordingly, a decrease in the viscosity results in a decrease in the ability of the fluid to lift particles. The pressure gradient increases because of the increase in concentration of solids in the lower part of the pipe.

Pipe-size effects

The intensity of turbulence is directly related to the pipe size. For a given mean velocity, the friction velocity decreases with increasing pipe diameter. Therefore, increase in the pipe diameter results in a decrease in the ability of the fluid to lift particles. This is demonstrated in Table 2, which lists data for 165 μm

(SA) sand particle slurries in three different pipe sizes: 5.15 cm, 26.3 cm, and 49.5 cm.

Comparisons of in situ profiles

The good agreement between the calculated and experimental average *in situ* solids and liquid velocities in Table 3 demonstrates that the model is capable of predicting component properties. [Experimental data are extracted from Scarlett and Grimley (1974).]

Conclusions

This study was performed in order to develop a model for flow of slurries through pipelines. Such flows are complex. Experimental measurement of the local velocity and concentration distributions in slurry flow is very difficult. Nonintrusive probes are limited, while internal probes interfere with the flow and cannot withstand the severe erosion resulting from the presence of solids. The modeling approach offers a meaningful, relatively inexpensive, complementary alternative for examining all useful details relating to slurry transport. The model developed in this work was found to give results which agreed very well with available pressure drop and velocity and concentration distribution data.

Acknowledgment

This work was supported by the National Science Foundation under Grant No. CBTE 8111258 and by the International Fine Particle Research Institute (IFPRI). The work on coal-water slurries was carried out with support under Grant No. DE-FG22-84PC70781 from the U.S. Department of Energy and also support from the State of Illinois Coal Development Board through the Center for Research on Sulfur in Coal. We are grateful for this support.

Notation

C = concentration, volume fraction
$\langle C \rangle$ = average concentration, volume fraction
$C_D = (4/3)gD(s-l)/v_\infty^2$, drag coefficient for free falling sphere
C_{max} = maximum packing concentration of solids, volume fraction
C_s = total solids concentration, volume fraction
D = inside diameter of pipe, m
d = diameter of solid particle, μm
$-dP/dz$ = pressure gradient, in Pa/m
Fr = modified Froude number, Eq. 22
f = Fanning friction factor for pipe flow
g = gravitational acceleration, m/s^2
N = number of particles per unit volume of slurry
R_{kl} = interactive force between component k and liquid phase, N
$R_{k(s-k)}$ = interactive force between solid component k and the remaining solids content, N
$Re = D\rho v/\mu$, Reynolds number for pipe
S_k = absolute roughness of the pipe, m
$s = \rho_s/\rho_l$, solid to liquid density ratio
v = velocity, m/s
$\langle v \rangle$ = mean velocity, m/s
v_y = vertical solid particle velocity, m/s
v_* = friction velocity, m/s
$\tilde{v}_{ky}$ = hypothetical vertical velocity of solid component k, m/s
y = distance from the bottom of the pipe, m

Greek letters

$\Lambda = N_{Re}C_D^{1/2}$
λ = coefficient of the support load, Eq. 45
ϵ_{ij} = turbulent eddy diffusivity tensor, m^2/s
ϵ_m = molecular diffusivity, m^2/s
ϵ_t = eddy diffusivity, m^2/s
κ = von Kármán's constant or the permeability, Eq. 27
μ = viscosity of liquid, kg/m · s
ν = kinematic viscosity of liquid, m^2/s
ν_t = eddy kinematic viscosity, m^2/s
ψ_{corr} = correction factor for mixing length
ψ_{damp} = van Driest damping function, Eq. 15
Φ_k = factor used in estimation of eddy kinematic viscosity of component k, Eq. 23
ϕ_l = factor used in estimation of eddy kinematic viscosity of liquid phase in the absence of interaction from the solid particles, Eq. 19
ϕ_k = factor used in estimation of eddy kinematic viscosity of component k in the absence of interaction from the other components, Eq. 20
ρ = density, kg/m^3
σ_k = Coulombic normal stress for component k, N/m^2
σ_t = turbulent Schmidt number
τ = shear stress, N/m^2
ω = hindered settling velocity of solids particles, m/s

Subscripts

dis = related to the pipe discharge
ins = related to the *in situ* condition

Literature Cited

Bagnold, R. A., "Experiments on a Gravity Free Dispersion of Large Solid Spheres in a Newtonian Fluid under Shear," *Proc. Roy. Soc. Lond.*, A(225), 49 (1954).

Bechteler, N., and K. Farber, "Stochastic Model of Suspended Solid Dispersion," *J. Hydraul. Eng.*, **111**(1), 64 (1985).

Boussinesq, J., "Essai sur la Théorie des Eaux Courantes," *Mém. Prés. Acad. Sci.*, **XXIII**, 46, Paris (1877).

Brinkman, H. C., "A Calculation on the Viscous Force Exerted by a Flowing Fluid on a Dense Swarm of Particles," *Appl. Sci. Res.*, **A1**, 27 (1947).

Cebeci, T., and A. M. O. Smith, *Analysis of Turbulent Boundary Layers*, Academic Press, New York (1974).

Colebrook, C. F., "Turbulent Flow in Pipes with Particular Reference to the Transition Region between the Smooth and Rough Pipe Laws," *J. Inst. Civil Eng.* (1939).

Danon H., M. Wolfshtein, and G. Hetsroni, "Numerical Calculations of Two-Phase Turbulent Round Jet," *Int. J. Multiphase Flow*, **3**, 223 (1977).

Dodge, D. W., and A. B. Metzner, "Turbulent Flow of Non-Newtonian Systems," *AIChE J.*, **5**, 189 (1959).

Drew, D. A., "Production and Dissipation of Energy in the Turbulent Flow of a Particle-Fluid Mixture, with Some Results on Drag Reduction," *J. Appl. Sci. Res.*, **98E**(4), 543 (1976).

van Driest, E. R., "On Turbulent Flow Near a Wall," *JAS*, **23**, 1007 (1956).

Genchev, Zh.D., and D. S. Karpuzov, "Effects of the Motion of Dust Particles on Turbulent Transport Equations," *J. Fluid Mech.*, **101**, 833 (1980).

Gillies, R., W. H. W. Husband, M. Small, and C. A. Shook, "Concentration Distribution Effects in a Fine-Particle Slurry," *Proc. Techn. Conf.*, Slurry Transport Assoc., 131 (Mar., 1983).

Happel, J., and H. Brenner, *Low Reynolds Number Hydrodynamics*, 2nd ed., Martinus Nijhoff Publishers, Hague, Netherlands (1983).

Hino, M., "Turbulent Flow with Suspended Particles," *Proc. ASCE*, **89**, HY4, (July, 1963).

Hinze, J. O., "Turbulent Fluid and Particle Interactions," *Prog. in Heat and Mass Transfer*, **6**, 433, Pergamon Press, New York (1972).

———, *Turbulence*, McGraw-Hill (1975).

Hsu, F. L., "Flow of Non-Colloidal Slurries in Pipelines, Experiments and Numerical Simulations," Ph.D. Thesis, Univ. of Illinois at Chicago (1987).

Kada, J., and T. J. Hanratty, "Effects of Solids in Turbulence in a Fluid," *AIChE J.*, **6**(4), 624 (1960).

Kazanskij, I., "Scale-Up Effects in Hydraulic Transport-Theory and Practice," *Paper B3, Hydrotransport 5*, 47 (1978).

Keska, J. K., "Fluctuations of the Solid Spatial Concentration in the Stationary Two-Phase Turbulent Flow of Heterogeneous Mixtures in Pipelines," *J. Pipelines*, **4**, 149 (1984).

Kril', S. I., "Concerning Methods for Writing Equations of Motion of Slurries," *Fluid Mech.-Soviet Res.*, **10**(6), 81 (1981).

Laufer, J., Nat. Advisory Comm. Aeronaut. Tech. Repts., No. 1174 (1954).
Lee, S. L. and F. Durst, "On the Motion of Particles in Turbulent Duct Flows," *Int. J. Multiphase Flow*, **8**(2), 125 (1982).
Ma, T-W., "Stability, Rheology and Flow in Pipes, Bends, Fittings, Valves and Venturi Meters of Concentrated Non-Newtonian Suspensions," Ph.D. Thesis, Univ. of Illinois at Chicago (1987).
Mahadevan, S., "Two-Phase Flows in Pipes," M.S. Thesis, Univ. of Kentucky, Lexington (Sept., 1984).
Metzner, A. B., and J. C. Reed, "Flow of Non-Newtonian Fluids—Correlations of the Laminar, Transition, and Turbulent-Flow Regions," *AIChE J.*, 430 (1955).
Nikuradse, J., "Gesetzmässigkeit der Turbulenten Strömung in Glattern Rohren," *Forschg. Arb. Ing.-Wes.*, No. 356 (1932).
Nunner, W., *VDI-Forschungsheft*, No. 455 (1956).
O'Brien, R. L., *Trans. Amer. Geophys. Union*, **14**, 487 (1933).
Ormancey, A., and J. Martinon, "Prediction of Particle Dispersion in Turbulent Flows," *PCH Physicochem. Hydrody. J.*, **5**(3/4), 229 (1984).
Owen, P. R., "Pneumatic Transport," *J. Fluid Mech.*, **39**(2), 407 (1969).
Pechenkin, M. V., "Experimental Studies of Flows with High Solid Particle Concentration," *Proc. Cong. A.I.R.H.*, Tokyo (1972).
Pourahmadi, F., and J. A. C. Humphrey, "Modeling Solid-Fluid Turbulent Flows with Application to Predicting Erosive Wear," *PCH Physicochem. Hydrody.*, **4**(3), 191 (1983).
Prandtl, L., *Führer durch die Strömungslehre*, 3rd ed., Braunschweig (1949).
Raudkivi, A. J., *Loose Boundary Hydraulics*, 2nd ed., Pergamon Press, New York (1975).
Richardson, J. F., and W. N. Zaki, "Sedimentation and Fluidization," *Trans. Inst. Chem. Eng.*, **32**(25) (1954).
Roco, M. C., and N. Balakrishnam, "Multi-Dimensional Flow Analysis of Solid-Liquid Mixtures," *J. of Rheol.*, **29**(4), 431 (1985).
Roco, M., and G. Frasineanu, "Metoda de Calcul Caracteristicilor de Curgere Ale Fluidelor Bifazate Lichid-Solid Prin Conducte Si Canale: I" *St. Cerc. Mec. Apl.*, TOM. 36, NR. 3, 311 (1977).
Roco, M. C., and S. Mahadevan, "Scale-Up Technique of Slurry Pipelines: 1. Turbulence," *J. of Energy Res. Technol.*, **108**, 269 (1986).
———, "Scale-Up Technique of Slurry Pipelines: 2. Numerical Integration," *J. of Energy Res. Technol.*, **108**, 278 (1986).
Roco, M. C., and C. A. Shook, "New Approach to Predict Concentration Distribution of Fine Particle Slurry Flows: I" *PCH Physicochem. Hydrody. J.*, **2**, spec. issue (1982).
———, "Modeling Slurry Flow, the Effect of Particle Size," *Can. J. Chem. Eng.*, **61**(4), 494 (1983).
———, "Turbulent Flow of Incompressible Mixtures," *J. of Fluids Eng.*, **107**, 224 (June, 1985).
Rubin, G., "Widerstands-und Auftriebsbeiwerte von rut enden, Kugelförmigen Partikeln in Stationären, Wandnahen Laminaren Grenzschichten," D. Eng. Diss., Univ. of Karlsruhe, Karlsruhe, West Germany (1977).
Saffman, P. G., "The Lift on a Small Sphere in a Slow Shear Flow," *J. Fluid Mech.*, **22**, 385 (1965).
Scarlett, B., and A. Grimley, "Particle Velocity and Concentration Profiles During Hydraulic Transport in a Circular Pipe," *Proc. Hydrotransport 3*, BHRA-Fluid Engineering, Cranfield, U.K., Paper D3, 23 (1974).
Scarlett, B., and M. G. Vinhas, "Concentration Profiles in the Horizontal Hydraulic Transport," Int. Conf. on Hydraulic Transport of Solids in Pipes, Paper D3, Rome, Italy (Oct., 1984).
Schriek, W., L. G. Smith, D. B. Haas, and W. H. W. Husband, "Experimental Studies on the Hydraulic Transport of Coal," Report E73-17, Saskatchewan Research Council, Saskatoon, Saskatchewan, Canada (Oct., 1973).
Shields, A., "Anwendung der Aehnlichkeits-Mechanik und der Turbulenzforschung auf die Geschiebebewegung, Preussische Versuchsanstalt fur Wasserban und Schiffbau," Berlin (1936).
Shook, C. A., and S. M. Daniel, "Flow of Suspensions of Solids in Pipeline: I. Flow with a Stable Stationary Deposit," *Can. J. Chem. Eng.*, **43**, 56 (1965).
Shook, C. A., R. Gillies, D. B. Haas, W. H. H. Husband, and M. Small, "Flow of Coarse and Fine Sand Slurries in Pipelines," *J. of Pipelines*, **3**, 13 (1982).
Soo, S. L., "Pipe Flow of A Dense Suspension," *J. Pipelines*, **6**, 193 (1987).
Soo, S. L., H. K. Ihrig, and A. F. El. Kough, "Experimental Determination of Statistical Properties of Two-Phase Turbulent Motion," *J. Basic Eng.*, **82D**(3), 609 (1960).
Tchen, C. M., "Mean Value and Correlation Problems Connected with the Motion of Small Particles Suspended in A Turbulent Fluid," Diss., Delft, Martinus, Nijhoff Publishers, Hague, Netherlands (1947).
Turian, R. M., and T. F. Yuan, "Flow of Slurries in Pipelines," *AIChE J.*, **23**, 232 (1977).
Wallis, G. B., *One-Dimensional Two-Phase Flow*, McGraw-Hill, New York (1969).
Yuu, S., "Diffusivities of Transferable Quantities in Turbulent Flow with Mean Velocity Distribution," *Phys. Fluids*, **28**(2) 466 (Feb., 1985).
Zisselmar, R., and O. Molerus, "Investigation of Solid-Liquid Pipe Flow with regard to Turbulent Modification," *Chem. Eng. J.*, **18**, 233 (1979).

Manuscript received Oct. 30, 1987, and revision received Oct. 18, 1988.